ISSN: pISSN 2976-1344 eISSN 2976-1352
AMC Multidisciplinary Research Journal (AMRJ)
Volume: 4 Issue: 1, Year 2025
****

A Novel Imidazole Derivative: Synthesis, Spectral Characterization, and DFT Study

Kamal Raj Sapkota[1], Jahanara Begam[2], Shilpi Kumari[3]

DOI: https://doi.org/10.3126/amrj.v4i1.78678

[1]Department of Chemistry, Tribhuvan University, Prithvi Narayan Campus, Pokhara, Nepal
[2]Department of Physics S.N.S. College, B.R.A. Bihar University, Muzaffarpur, Bihar, India
[3]University Department of Chemistry, B. R. A. Bihar University, Muzaffarpur, Bihar, India
[1]Corresponding Author, Email: sapkotakamal69@gmail.com
Article History: Received: Jan. 10, 2025 Revised: April. 4, 2025 Received: May. 5, 2025

Abstract

A novel Imidazole derivative, (E)-N-((1H-indol-7-yl) methylene)-5-phenyl-1H-imidazol-2-amine (IPA), was synthesized and characterized by elemental analysis, FT-IR, NMR, UV–Vis, and mass spectrometry. Spectral data confirmed the structure and purity of the compound. UV–Vis analysis showed π→π* and n→π* transitions, indicating strong conjugation. The molecular ion peak at m/z 286.12 verified its molecular weight. DFT study at the B3LYP/6-311G(d,p) level exhibits a HOMO–LUMO gap of 2.80 eV, in good agreement with the experimental value (2.70 eV), supporting its electronic structure and optoelectronic potential.

Keywords: Imidazole, Transitions, Conjugation, DFT, HOMO

Introduction

Heterocyclic compounds are of immense significance in medicinal and materials chemistry due to their multifarious biological and physicochemical characteristics (Kabir et al., 2022; Baranwal et al., 2023). Among these, imidazole derivatives hold a foremost place owing to their vast applications in pharmaceuticals, agrochemicals, and functional materials. Imidazole, a five-membered nitrogen-containing heterocycle, displays impressive biological actions, including antifungal, antibacterial, anticancer, anti-inflammatory, and antiviral effects (Kabir et al., 2022; Baranwal et al., 2023; Karthikeyan et a., 2023; Hossain et al., 2018). These characteristics have made imidazole-based compounds a focal point of research in drug discovery and chemical synthesis. The importance of imidazole derivatives extends beyond biological applications (Zhang et al., 2014; Gaba et al., 2016; Tolomeu et al., 2023). They play a vital role in coordination chemistry, catalysis, and polymer science, additionally improving their synthetic and industrial applicability (Gaba et al., 2016; Tolomeu et al., 2023; Engel et al., 2020). Their capacity to act as ligands for transition metal complexes and participate in hydrogen bonding makes them valuable in supramolecular chemistry and material sciences (Engel et al., 2020; Sauvage, 2008; Carboni et al., 2011). Thus, the synthesis and characterization of novel imidazole derivatives remain a pivotal area of research, aspiring to examine their structural diversity and functional properties (Kabir et al., 2022; Baranwal et al., 2023; Karthikeyan et a.,

2023; Hossain et al., 2018; Zhang et al., 2014; Gaba et al., 2016; Tolomeu et al., 2023; Engel et al., 2020; Sauvage, 2008; Carboni et al., 2011). Classic methods for imidazole synthesis typically concern the condensation of 1,2-dicarbonyl compounds with aldehydes and amines under acidic or basic conditions (Carboni et al., 2011; Shitole, 2020; Kumar et al., 2021; Mirallai, 2015). Nevertheless, advancements in synthetic processes have introduced green chemistry procedures, microwave-assisted synthesis, and solvent-free reactions, presenting improved yields, decreased reaction times, and environmental sustainability. The incorporation of diverse substituents on the imidazole ring improves the physicochemical effects of the resulting compounds, extending their potential applications in medicinal chemistry and materials science. Recent focus in research has highlighted the modification of imidazole derivatives to improve their pharmacological efficacy. Modifying their structural composition, especially by introducing electron-donating or electron-withdrawing groups, is pivotal in modulating their biological action.

Again, incorporating the imidazole framework with other pharmacophores, such as quinoline, benzothiazole, or pyrimidine, has contributed to the development of novel therapeutic agents with improved efficacy (Kabir et al., 2022; Baranwal et al., 2023; Karthikeyan et a., 2023; Hossain et al., 2018; Zhang et al., 2014; Gaba et al., 2016; Tolomeu et al., 2023; Engel et al., 2020; Sauvage, 2008; Carboni et al., 2011; Shitole, 2020; Kumar et al., 2021; Mirallai, 2015). This study focuses on the synthesis and structural study of a new imidazole derivative ((E)-N-((1H-indol-7-yl) methylene)-5-phenyl-1H-imidazol-2-amine (IPA)) utilizing a well-defined synthetic method. Structural characterization of the synthesized compound is carried out employing diverse spectroscopic approaches, including FT-IR (Fourier-transform infrared) spectroscopy, UV-Vis spectroscopy, NMR (nuclear magnetic resonance) spectroscopy, and mass spectrometry (MS). These analytical tools furnish vital understandings of the molecular architecture, functional group exchanges, and purity of the compound, ensuring its structural integrity. The synthesized imidazole derivative (IPA)) is expected to exhibit promising pharmacological properties, warranting further biological evaluations. The results from this investigation will contribute to the growing body of knowledge in imidazole chemistry and could enable the design of new bioactive molecules. The rational effect of such heterocyclic compounds enriches our comprehension of their chemical behavior and spreads the groundwork for future innovations in drug development and material science.

Methods and Materials

Methods

The Fourier-transform infrared (FT-IR) spectrum of ((E)-N-((1H-indol-7-yl) methylene)-5-phenyl-1H-imidazol-2-amine (IPA) was recorded at 25 °C using a Perkin-Elmer FT-IR spectrometer to identify functional groups and analyze vibrational characteristics. The molecular framework of carbon and hydrogen was examined through ^{13}C and ^{1}H nuclear magnetic resonance (NMR) spectroscopy using a Bruker AVANCE-III spectrometer. The electronic absorption behavior of the compound was investigated via ultraviolet-visible (UV-Vis) spectroscopy on a Perkin-Elmer Lambda 35 spectrometer, spanning the 200–750 nm wavelength range with a 1 nm bandwidth. Electrospray ionization mass spectrometry (ESI-MS) was conducted on a WATERS Q-ToF Premier Mass Spectrometer to determine the molecular ion and fragmentation pattern. Additionally, the elemental composition of the compound was confirmed

using a Perkin-Elmer 2400 Series II CHNS/O Analyzer, ensuring consistency with theoretical calculations.

Materials

For the synthesis of ((E)-N-((1H-indol-7-yl) methylene)-5-phenyl-1H-imidazol-2-amine (IPA), all required chemicals were purchased from Sigma-Aldrich and utilized without undergoing any purification process.

Computational details

Theoretical studies were accomplished using Gaussian 09 (Frisch et al., 2010) and GaussView (Dennington et al., 2007) software, employing the density functional theory (DFT) approach with the B3LYP functional and the 6-311G(d,p) basis set (Jamal et al., 2024; 2025).

Results

Synthesis of (E)-N-((1H-indol-7-yl) methylene)-5-phenyl-1H-imidazol-2-amine (IPA)

The compound IPA was prepared through the reaction of 5-phenyl-1H-imidazol-2-amine (2) with 1H-indole-7-carbaldehyde (1), as depicted in Scheme 1. Initially, 0.50 g (3.14 mmol) of 5-phenyl-1H-imidazol-2-amine was dissolved in 20 mL of methanol. To this solution, 0.45 g (3.10 mmol) of 1H-indole-7-carbaldehyde was gradually introduced. The reaction mixture was refluxed for 5 hours, resulting in the appearance of a light yellow precipitate, while the volume of the solution was reduced to 10 mL. The solid outcome was collected via filtration, entirely washed with 5 mL of cold methanol, followed by 10 mL of hexane, and recrystallized using methanol. Finally, the purified compound, IPA, was dried in a vacuum desiccator, yielding 0.80 g of yellow solid with an 84% yield. The elemental analysis of (E)-N-((1H-indol-7-yl) methylene)-5-phenyl-1H-imidazol-2-amine (IPA) (Chemical Formula: $C_{18}H_{14}N_4$) was accomplished to ensure its composition. The calculated percentages for carbon, hydrogen, and nitrogen were 75.50%, 4.93%, and 19.57%, respectively. The experimental values were found to be 75.10% for carbon, 4.78% for hydrogen, and 19.23% for nitrogen. The close agreement between the theoretical and experimental values confirms the molecular integrity and purity of the synthesized compound. Moreover, Figure 1 presents the structure of IPA.

ISSN: pISSN 2976-1344 eISSN 2976-1352
AMC Multidisciplinary Research Journal (AMRJ)
Volume: 4 Issue: 1, Year 2025
****

Figure 1

Structure of IPA

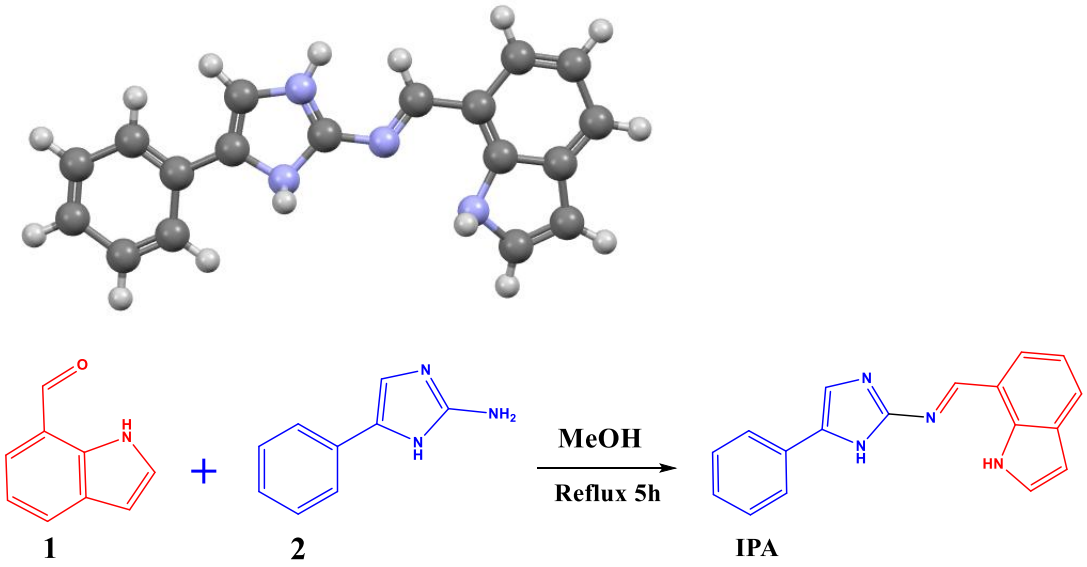

Scheme 1

NMR

The ^{1}H NMR spectrum (Figure 2) of (E)-N-((1H-indol-7-yl) methylene)-5-phenyl-1H-imidazol-2-amine (IPA) exhibits characteristic proton signals corresponding to different functional groups within the molecule. A singlet at δ 10.0 ppm corresponds to the NH proton of the indole ring, which is deshielded due to hydrogen bonding or aromatic effects (Pavia et al., 2015; Pretsch et al., 2013; Sharma, 2007). In the region δ 9.0–8.0 ppm, three distinct peaks are marked. A singlet in this region probably appears from the imine (-CH=N) proton (Pavia et al., 2015; Sharma, 2007), while a doublet and a multiplet illustrate aromatic protons, perhaps from the indole or imidazole ring system. Further downfield, another set of three peaks is noted in the δ 8.0–7.0 ppm range: a singlet, a triplet, and a doublet. These peaks are attributed to different aromatic protons, most presumably from the phenyl and imidazole rings, with the triplet exhibiting a proton experiencing equal coupling from adjacent protons (Pavia et al., 2015; Pretsch et al., 2013; 2000; Sharma, 2007). In the δ 7.0–6.0 ppm region, a doublet arises, which is characteristic of an aromatic proton in an electron-rich environment, possibly from the imidazole or phenyl system (Pavia et al., 2015; Pretsch et al., 2013; 2000). Further, a solvent (DMSO-d_6) peak is marked between the δ 4.0–3.0 ppm. Overall, the ^{1}H NMR spectrum provides structural insights into the molecular framework, confirming the presence of key functional groups through distinct chemical shifts and coupling patterns.

The ^{13}C NMR spectrum (Figure 2) of (E)-N-((1H-indol-7-yl) methylene)-5-phenyl-1H-imidazol-2-amine (IPA) shows two peaks in the δ 160–165 ppm region, corresponding to highly deshielded imine and imidazole carbons (Pretsch et al., 2013; 2000; Sharma, 2007). Four peaks appear in the δ 140–130 ppm range, attributed to quaternary aromatic carbons from the indole, imidazole, and phenyl rings. Five peaks are noticed within δ 130–120 ppm range, with one appearing broader, revealing overlapping signals from protonated aromatic carbons (Pavia et al.,

2015; Pretsch et al., 2013; 2000; Sharma, 2007). Two different peaks correspond to additional aromatic carbons in the δ 120–110 ppm region. Another peak appears in the δ 110–100 ppm range, associated with a more shielded carbon (Pavia et al., 2015; Sharma, 2007). Finally, a solvent peak at δ 40–30 ppm corresponds to DMSO-d_6, usually utilized in NMR examination. The overall spectral pattern demonstrates the existence of imine, indole, imidazole, and phenyl carbons, supporting the structural identity of the compound.

Figure 2

NMR for IPA

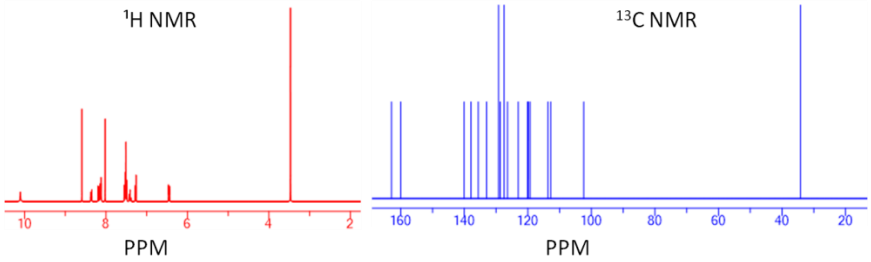

FT-IR

The FT-IR spectrum (Figure 3) of (E)-N-((1H-indol-7-yl) methylene)-5-phenyl-1H-imidazol-2-amine furnishes essential details regarding the functional groups present in the molecule, demonstrating its structural integrity. A broad and medium-intensity band observed at 3132 cm^{-1} is characteristic of the N–H stretching vibration, indicative of the indole and imidazole NH groups (Pavia et al., 2015; Pretsch et al., 2013; 2000; Ahmad et al., 2018; Socrates, 2004; Sharma, 2007). The peak at 3059 cm^{-1} corresponds to aromatic C–H stretching vibrations, which confirms the presence of multiple aromatic systems, including the phenyl, indole, and imidazole rings (Pavia et al., 2015; Socrates, 2004; Sharma, 2007). A weak absorption at 2772 cm^{-1} is likely due to C–H stretching of the imine group or a weak overtone band (Pavia et al., 2015; Socrates, 2004). A prominent band at 1674 cm^{-1} is assigned to the C=N stretching vibration of the imine (azomethine) linkage, a key feature of the Schiff base structure (Pavia et al., 2015; Pretsch et al., 2013; 2000; Socrates, 2004). Additional bands observed at 1614, 1592, 1584, and 1528 cm^{-1} are attributed to C=C and C=N stretching vibrations in the aromatic and heterocyclic systems, reflecting conjugation within the π-system of the molecule (Pavia et al., 2015; Socrates, 2004; Sharma, 2007). The bands at 1488, 1482, and 1448 cm^{-1} are due to C–H in-plane bending vibrations and aromatic ring skeletal motions. Absorptions at 1395, 1372, and 1351 cm^{-1} suggest the presence of C–N stretching vibrations and deformation modes typical of substituted heterocycles such as imidazole and indole. Peaks at 1316, 1277, and 1251 cm^{-1} are attributed to aromatic C–N stretching and in-plane C–H deformation vibrations. Further, the bands at 1210, 1172, and 1131 cm^{-1} support the presence of C–H wagging and skeletal vibrational modes within the aromatic systems (Pavia et al., 2015; Socrates, 2004; Sharma, 2007). The region between 1102–1009 cm^{-1} shows bands at 1102, 1073, 1039, and 1009 cm^{-1}, which can be attributed to aromatic ring breathing and C–N skeletal vibrations (Pavia et al., 2015; Pretsch et al., 2013; Socrates, 2004). The bands at 959, 917, 845, and 830 cm^{-1} are

consistent with C–H out-of-plane bending of mono- and disubstituted aromatic rings (Socrates, 2004; Sharma, 2007). Further support for aromatic substitution patterns is evident from the peaks at 755, 729, 693, and 659 cm^{-1}, which reflect out-of-plane deformations of the phenyl and indole systems [19-23]. Finally, the low-frequency bands at 599, 557, and 455 cm^{-1} are assigned to ring deformation and skeletal torsional modes of the heterocyclic framework (Pavia et al., 2015; Socrates, 2004; Sharma, 2007). Overall, the FT-IR data strongly support the proposed molecular structure and successful formation of the Schiff base.

Figure 3

FT-IR for IPA

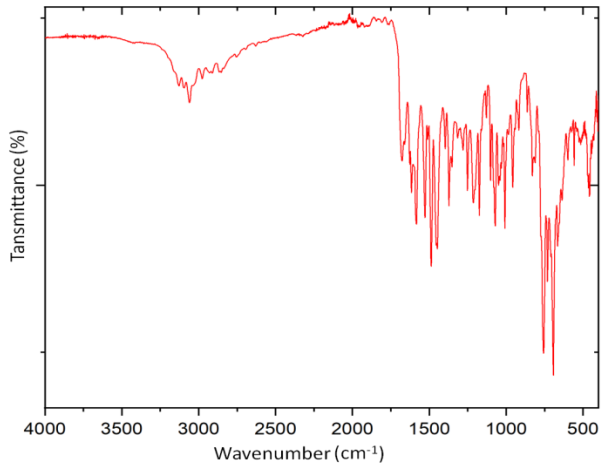

UV-Vis

The UV-Vis spectrum (Figure 4) for (E)-N-((1H-indol-7-yl) methylene)-5-phenyl-1H-imidazol-2-amine, recorded in DMSO displays two absorption bands that provide significant insights into its electronic structure and conjugation. A small peak at 345 nm is designated to a π→π* electronic transition (Pavia et al., 2015; Socrates, 2004; Sharma, 2007). This transition is mainly localized within the aromatic moieties of the molecule, including the indole, imidazole, and phenyl rings. These rings possess delocalized π-electrons, and their overlap leads to electronic excitation within the π-system. This band's moderate intensity proposes a localized excitation nature with limited charge transfer. A more intense and broader absorption band is recorded at 459 nm, which is attributed to an n→π* transition (Pretsch et al., 2013; 2000; Sharma, 2007). This transition affects the excitation of a non-bonding electron (n) from the nitrogen atom of the azomethine (–CH=N–) group to an antibonding π* orbital (Pavia et al., 2015; Sharma, 2007). The existence of this peak at a longer wavelength (red-shifted) reflects the influence of the extended conjugation in the molecule, spanning across the indole, imine, and imidazole units (Pavia et al., 2015; Pretsch et al., 2013; 2000; Ahmad et al., 2018; Sharma, 2007). The intense absorption at this wavelength also suggests the occurrence of intramolecular charge transfer (ICT), enabled by the conjugated π-system and the presence of electron-donating and electron-withdrawing groups within the molecule (Pavia et al., 2015; Pretsch et al., 2013; Sharma, 2007). The occurrence of the absorption band at 459 nm, which lies in the visible region, provides the compound a potential for chromophoric and optoelectronic behavior,

implying probable applications in photophysical systems. The bathochromic shift (longer wavelength absorption) corresponded to simple Schiff bases, supporting the notion of enhanced electron delocalization throughout the molecular scaffold (Pavia et al., 2015; Pretsch et al., 2013; 2000; Ahmad et al., 2018; Sharma, 2007). Overall, the UV–Vis spectrum demonstrates the existence of conjugated π-systems and electronic transitions familiar with Schiff base derivatives with heterocyclic aromatic systems, supporting the structure and purity of the synthesized compound.

Figure 4

UV–Vis for IPA

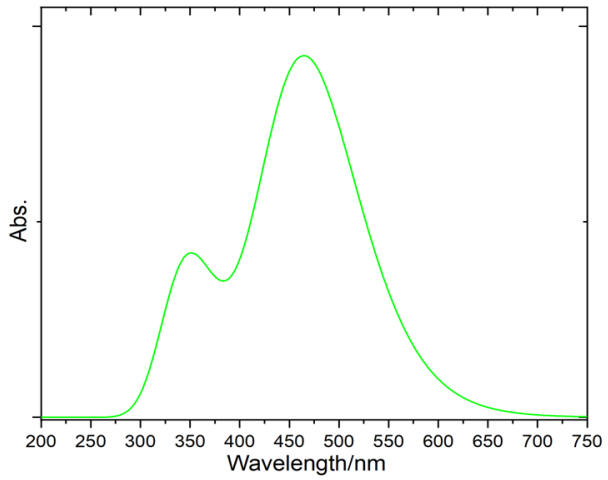

Mass Spectrometry (ESI-MS or EI-MS)

The mass spectrum for (E)-N-((1H-indol-7-yl) methylene)-5-phenyl-1H-imidazol-2-amine indicates a molecular ion peak (M^+) at m/z 286.12, which corresponds to the molecular weight of the compound and confirms its molecular formula. This peak appears as the base peak (100% relative intensity), indicating high stability and abundance of the parent ion under the ionization conditions. In addition to the molecular ion, isotopic peaks are observed at m/z 287.13 (19.6%), m/z 288.13 (1.8%), and m/z 287.12 (1.5%), which correspond to the natural isotopic distribution of the constituent elements, primarily due to ^{13}C and ^{2}H (D) or ^{15}N isotopes. The peak at m/z 287.13 represents the $[M+1]^+$ ion and arises mainly from the presence of ^{13}C isotopes in the molecule, with a relative abundance consistent with a compound containing approximately 18–20 carbon atoms. The minor peak at m/z 288.13 is attributed to the $[M+2]^+$ ion, likely resulting from the presence of two ^{13}C atoms or a combination of ^{13}C and other heavier isotopes (e.g., ^{2}H, ^{15}N) in the molecular ion. The low-intensity peak at m/z 287.12 (1.5%) may be a result of a slight overlapping of isotope contributions or fragment ions formed under soft ionization conditions. The absence of major fragment peaks and the dominance of the molecular ion peak suggest that the compound remains largely intact, indicative of high molecular stability, typical in Schiff bases and aromatic heterocycles under ESI or EI conditions. This mass spectral pattern confirms the molecular mass and purity of the compound and supports the proposed molecular structure based on its elemental composition and isotopic signature.

HOMO–LUMO Energy Gap (Theoretical vs. Experimental)

The experimental energy gap, derived from the maximum absorption wavelength (λmax = 459 nm) in the UV–Vis spectrum, is around 2.70 eV, based on the relation ΔE = 1240/λ (Pavia et al., 2015; Atkins et al., 2023; Sharma, 2007). This value corresponds to the optical band gap, indicating the electronic excitation from the ground state to the excited state, including solvent and vibrational relaxation effects. The theoretical HOMO–LUMO gap (Figure 5) obtained from DFT calculations is 2.80 eV, which designates the electronic energy difference between the frontier molecular orbitals in the ground state geometry. The tiny overestimation of the theoretical gap compared to the experimental value is normally observed and could be attributed to the absence of solvent and vibronic interactions in the computational model, as well as the limits of the functional and basis set used in DFT (Jamal et al., 2025; Medel et al., 2021). The comparable agreement between the experimental (2.70 eV) and computed (2.80 eV) values implies that the theoretical model is reliable and supports the existence of an extended π-conjugated system with efficient intramolecular charge transfer (ICT). Such a gap magnitude also proposes potential applications in optoelectronic and photophysical materials.

Figure 5

Calculated HOMO–LUMO gap for IPA

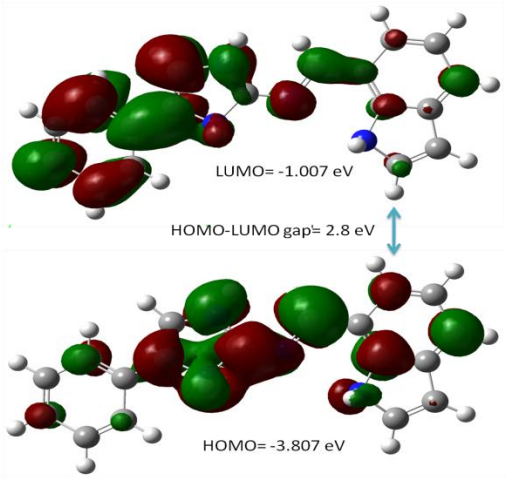

Conclusions

This study reveals the successful synthesis and thorough characterization of a novel Imidazole derivative, IPA. The integration of spectral techniques furnished a clear understanding of its molecular structure, ensuring the successful formation of the imine linkage and the presence of key functional groups. Notably, the UV–Vis and mass spectral data indicated significant electronic effects and molecular stability. Theoretical DFT computations complemented the experimental results, with the HOMO–LUMO gap proposing a well-conjugated system capable for intramolecular charge transfer. These outcomes not only validate

the molecular design but also highlight the potential of IPA for further investigation in materials science and electronic applications.

References

Ahmad, M. S., Khalid, M., Shaheen, M. A., Tahir, M. N., Khan, M. U., Braga, A. A. C., & Shad, H. A. (2018). Synthesis and XRD, FT-IR vibrational, UV–vis, and nonlinear optical exploration of novel tetra substituted imidazole derivatives: A synergistic experimental-computational analysis. Journal of Physics and Chemistry of Solids, 115, 265–276.

Atkins, P. W., De Paula, J., & Keeler, J. (2023). Atkins' physical chemistry. Oxford University Press.

Baranwal, J., Kushwaha, S., Singh, S., & Jyoti, A. (2023). A review on the synthesis and pharmacological activity of heterocyclic compounds. Current Physical Chemistry, 13(1), 2–19.

Carboni, S., Gennari, C., Pignataro, L., & Piarulli, U. (2011). Supramolecular ligand–ligand and ligand–substrate interactions for highly selective transition metal catalysis. Dalton Transactions, 40(17), 4355–4373.

Dennington, R. D. II, Keith, T., & Millam, J. (2007). GaussView (Version 4.1.2). Semichem Inc.

Engel, E. R., & Scott, J. L. (2020). Advances in the green chemistry of coordination polymer materials. Green Chemistry, 22(12), 3693–3715.

Frisch, M. J., Trucks, G. W., Schlegel, H. B., Scuseria, G. E., Robb, M. A., Cheeseman, J. R., Scalmani, G., Barone, V., Mennucci, B., Petersson, G. A., et al. (2010). Gaussian 09 Revision E.01. Gaussian, Inc.

Gaba, M., & Mohan, C. (2016). Development of drugs based on imidazole and benzimidazole bioactive heterocycles: Recent advances and future directions. Medicinal Chemistry Research, 25, 173–210.

Hossain, M., & Nanda, A. K. (2018). A review on heterocyclic: Synthesis and their application in medicinal chemistry of imidazole moiety. Science, 6(5), 83–94.

Jamal, A., & Faizi, M. S. H. (2024). Synthesis, structural characterization, DFT calculations, and molecular docking of a novel quinoline derivative. Journal of Molecular Structure, 1300, 137251.

Jamal, A., Faizi, M. S. H., & Ferjani, H. (2025). Designing of quinoline-based esterase inhibitor: Synthesis, crystal structure, DFT calculations, and molecular docking. Journal of Molecular Structure, 1319, 139540.

Kabir, E., & Uzzaman, M. (2022). A review on biological and medicinal impact of heterocyclic compounds. Results in Chemistry, 4, 100606.

Karthikeyan, S., Grishina, M., Kandasamy, S., Mangaiyarkarasi, R., Ramamoorthi, A., Chinnathambi, S., ... & John Kennedy, L. (2023). A review on medicinally important heterocyclic compounds and importance of biophysical approach of underlying the insight mechanism in biological environment. Journal of Biomolecular Structure and Dynamics, 41(23), 14599–14619.

Kumar, A., Rasool, J., & Ahmed, Q. N. (2021). Chemistry of 2-oxoaldehydes and 2-oxoacids. Elsevier.

Medel, R., & Suhm, M. A. (2021). Predicting OH stretching fundamental wavenumbers of alcohols for conformational assignment: Different correction patterns for density

functional and wave-function-based methods. Physical Chemistry Chemical Physics, 23(9), 5629–5643.

Mirallai, S. I. (2015). New chemistry of N'-arylbenzamidines.

Pavia, D. L., Lampman, G. M., Kriz, G. S., & Vyvyan, J. R. (2015). Introduction to spectroscopy.

Pretsch, E., Bühlmann, P., & Affolter, C. (2000). Structure determination of organic compounds. Springer-Verlag.

Pretsch, E., Clerc, T., Seibl, J., & Simon, W. (2013). Tables of spectral data for structure determination of organic compounds. Springer Science & Business Media.

Sauvage, J. P. (Ed.). (2008). Transition metals in supramolecular chemistry. John Wiley & Sons.

Sharma, Y. R. (2007). Elementary organic spectroscopy. S. Chand Publishing.

Shitole, N. V. (2020). An environmentally benign synthesis of 2,4,5-triaryl-1H-imidazoles via multi-component reactions and its medicinal importance. In Green Chemistry and Sustainable Technology (pp. 213–233). Apple Academic Press.

Socrates, G. (2004). Infrared and Raman characteristic group frequencies: Tables and charts. John Wiley & Sons.

Tolomeu, H. V., & Fraga, C. A. M. (2023). Imidazole: Synthesis, functionalization and physicochemical properties of a privileged structure in medicinal chemistry. Molecules, 28(2), 838.

Zhang, L., Peng, X. M., Damu, G. L., Geng, R. X., & Zhou, C. H. (2014). Comprehensive review in current developments of imidazole-based medicinal chemistry. Medicinal Research Reviews, 34(2), 340–437.